The thermal history of the Miocene Ibar Basin (Southern Serbia): new constraints from apatite and zircon fission track and vitrinite reflectance data

NEVENA ANDRIĆ[1]✉, BERNHARD FÜGENSCHUH[2], DRAGANA ŽIVOTIĆ[1] and VLADICA CVETKOVIĆ[1]

[1]University of Belgrade, Faculty of Mining and Geology, Đušina 7, 11000 Belgrade, Serbia;
✉nevena.andric@rgf.bg.ac.rs; dragana.zivotic@rgf.bg.ac.rs; cvladica@rgf.bg.ac.rs
[2]University of Innsbruck, Faculty of Geo- and Atmospheric Sciences, Institute of Geology, Innrain 52f, 6020 Innsbruck, Austria;
bernhard.fuegenschuh@uibk.ac.at

Abstract: The Ibar Basin was formed during Miocene large scale extension in the NE Dinaride segment of the Alpine-Carpathian-Dinaride system. The Miocene extension led to exhumation of deep seated core-complexes (e.g. Studenica and Kopaonik core-complex) as well as to the formation of extensional basins in the hanging wall (Ibar Basin). Sediments of the Ibar Basin were studied by apatite and zircon fission track and vitrinite reflectance in order to define thermal events during basin evolution. Vitrinite reflectance (VR) data (0.63–0.90 %Rr) indicate a bituminous stage for the organic matter that experienced maximal temperatures of around 120–130 °C. Zircon fission track (ZFT) ages indicate provenance ages. The apatite fission track (AFT) single grain ages (45–6.7 Ma) and bimodal track lengths distribution indicate partial annealing of the detrital apatites. Both vitrinite reflectance and apatite fission track data of the studied sediments imply post-depositional thermal overprint in the Ibar Basin. Thermal history models of the detrital apatites reveal a heating episode prior to cooling that began at around 10 Ma. The heating episode started around 17 Ma and lasted 10–8 Ma reaching the maximum temperatures between 100–130 °C. We correlate this event with the domal uplift of the Studenica and Kopaonik cores where heat was transferred from the rising warm footwall to the adjacent colder hanging wall. The cooling episode is related to basin inversion and erosion. The apatite fission track data indicate local thermal perturbations, detected in the SE part of the Ibar basin (Piskanja deposit) with the time frame ~7.1 Ma, which may correspond to the youngest volcanic phase in the region.

Key words: Balkan Peninsula, Ibar Basin, low-temperature thermochronology, core-complex, basin inversion, organic matter.

Introduction

The process of lithospheric extension is characterized by exhumation of middle to lower continental crust along crustal-scale detachments (Lister & Davis 1989). The exhumation of the high-grade metamorphic rocks in the footwall of the detachment is followed by subsidence and development of sedimentary (supra-detachment) basins on the hanging wall (Friedmann & Burbank 1995).

In general, the thermal evolution of supra-detachment basins is influenced by the interplay of several factors related to detachment activity: i) temperature contrast between the rapidly exhuming warm footwall and the cold hanging wall; ii) burial history of the basin; iii) magmatism ± hydrothermal activity and iv) basin inversion and exhumation (Dunkl et al. 1998; Kounov et al. 2004; Márton et al. 2010). The thermal state of the supradetachment basins is potentially affected by rapid exhumation of the warm footwall along the detachment. The heat advection leads to an elevated thermal gradient in the footwall and, subsequently, this heating was transferred by conduction to the hanging wall (Grasemann & Mancktelow 1993).

The Miocene Ibar Basin is located 200 km south of Belgrade, covering an area of approximately 320 km² (Fig. 1). It is a northwest-southeast elongated tectonic depression with a maximum length of 20 km and width of 12 km.

The Ibar Basin is supra-detachment basin, which provides the opportunity to study the thermal influence of the exhuming core on the basin fill in the hanging wall of the active detachment. The Ibar Basin belongs to the group of Lower Miocene intramontane basins called the Dinaridic lake system (Krstić et al. 2003; Harzhauser & Mandić 2008). The formation of these basins was contemporaneous with the extensional collapse of the Alpine orogenic wedge and back-arc Pannonian extension in the Miocene (Tari et al. 1992; Ilić & Neubauer 2005; Horváth et al. 2006; Leew et al. 2012), which was accompanied by exhumation of the metamorphic core-complexes (Tari et al. 1999; Ustaszewski et al. 2010; Matenco & Radivojević 2012; Stojadinović et al. 2013). The subsidence of the hanging wall of these detachments was accompanied by the formation of basins on the top.

Previous studies of the Ibar Basin were related mostly to stratigraphy, and exploration of mineral resources (coal, boron minerals, and magnesite). However, none of the earlier studies focused on elucidating the basin's evolution in more detail, especially in terms of its high heat flow regime. This study aims at providing new information about the thermal history of the Ibar Basin. Additionally, our data shed light on
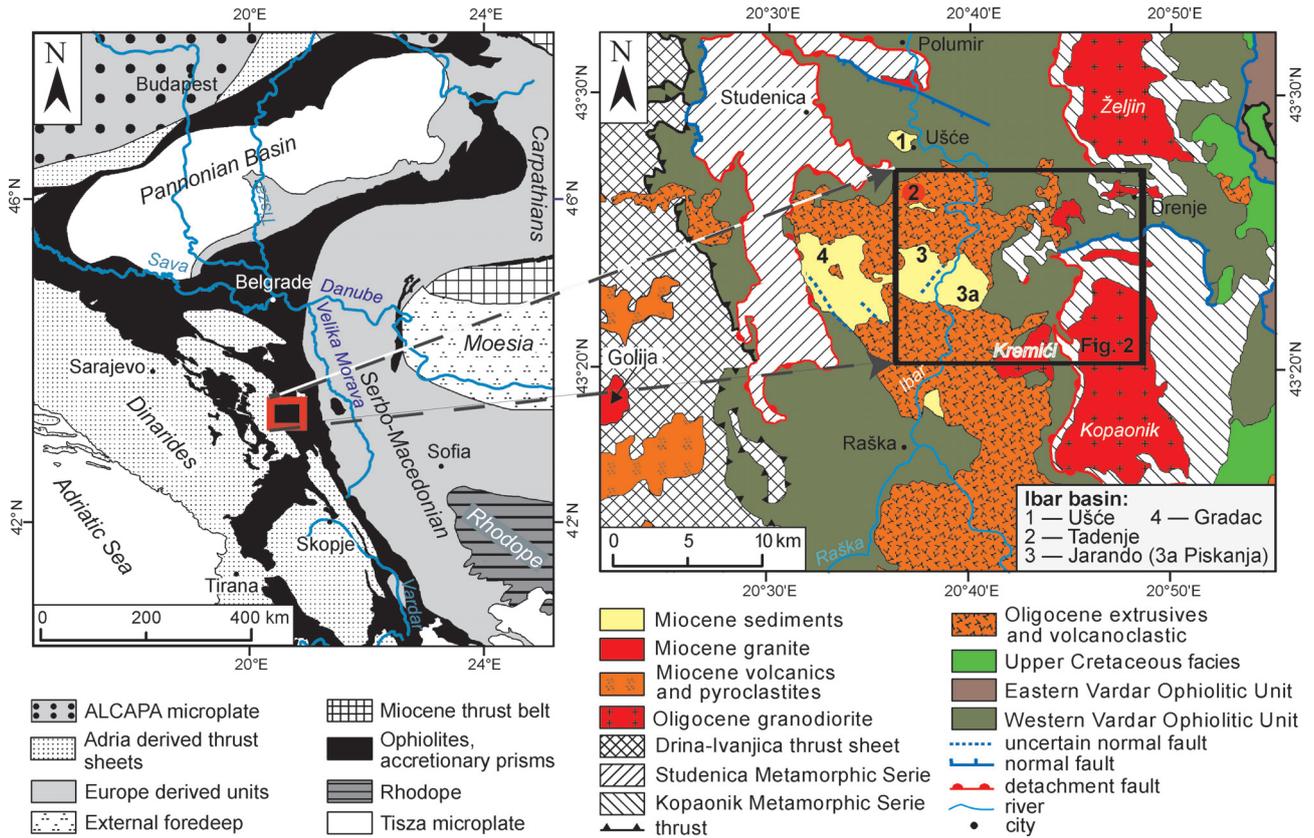
Fig. 1. Tectonic map of the Balkan Peninsula (modified after Schmidt et al. 2008), geological map of the study area (after Schefer 2010) and Basic Geological Map of Serbia, 1:100,000; Sheets Novi Pazar (Urošević et al. 1970a), Vrnjci (Urošević et al. 1970b), Sjenica (Mojsilović et al. 1978) and Ivanjica (Brković et al. 1976).
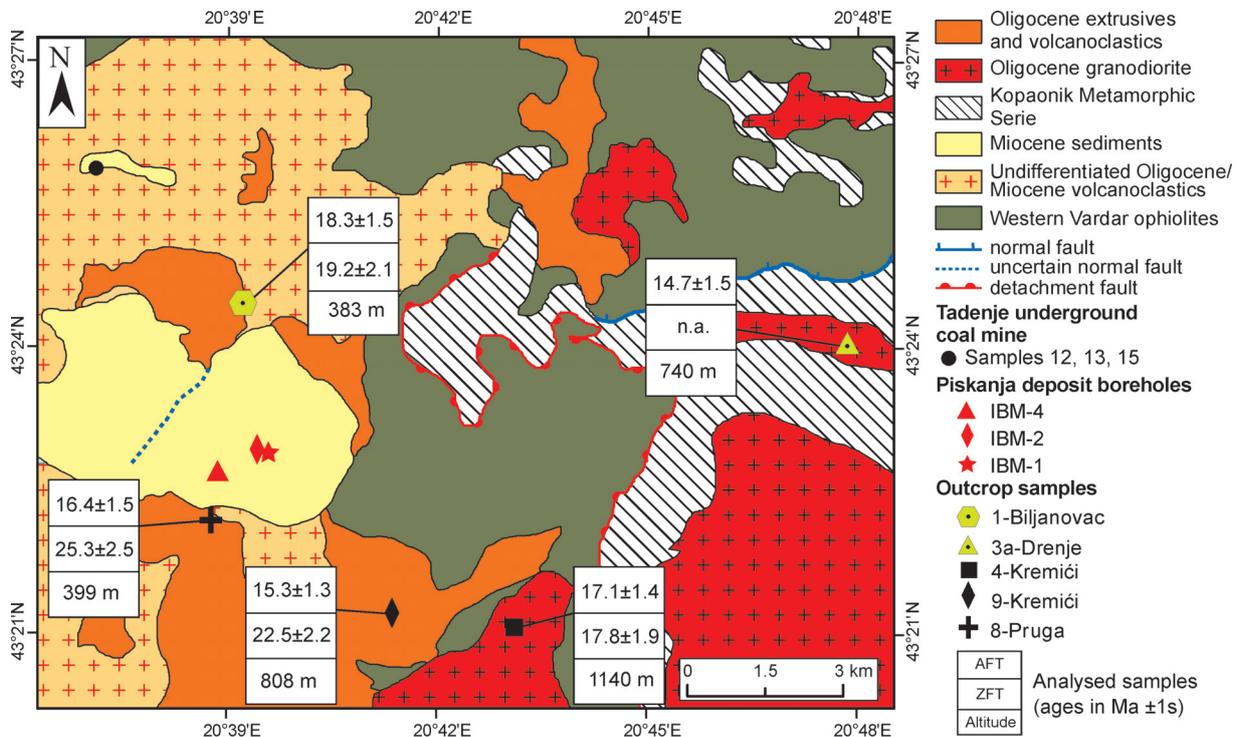

Fig. 2. Sampling location with new zircon and apatite fission track data for the surface samples.

the time and magnitude of paleo-thermal episodes in the Ibar Basin, including the phases of basin inversion and regional uplift (i.e. exhumation).

Geological setting

The Ibar Basin belongs to the eastern/south-eastern parts of the inner Dinarides (Fig. 1). It is situated on top of a Late Cretaceous to Eocene Adria-derived nappe stack which formed in the course of the Adria-Europe collision (Schmid et al. 2008). The collision was preceded by ophiolite obduction onto the distal Adriatic continental margin during the Late Jurassic as well as by subsequent closure of the last Neotethys oceanic realm forming the Sava suture zone (Pamić et al. 2002; Schmid et al. 2008; Ustaszewski et al. 2009). Later on, the ophiolites were involved in out-of-sequence thrusting forming composite nappes along with the Adria derived continental units in the lower position. The composite nappes namely the Drina-Ivanjica and Jadar-Kopaonik units consist of nonmetamorphosed to slightly metamorphosed Upper Paleozoic–Lower Jurassic sediments of the distal Adria margin overlain by Late Jurassic ophiolites (Fig. 1 — Dimitrijević 1997; Karamata 2006; Schmid et al. 2008; Schefer et al. 2010).

In the Ibar area these composite nappes are represented by the Kopaonik Metamorphic Series or Jadar-Kopaonik composite nappe (Fig. 1). During the Late Oligocene post-orogenic phase these series were intruded by the I-type granitoids of Drenje (31.7–31.2 Ma — Schefer et al. 2011) and Kopaonik (30.9–30.7 Ma — Schefer et al. 2011). The dacite- andesite extrusions and volcanoclastic rocks (31 Ma — Cvetković et al. 1995) intruded and/or overlaid ophiolites (Cvetković et al. 1995; Schefer et al. 2011). In the Miocene the study area underwent N-S extension (Schefer 2010), which led to the exhumation of the Studenica and Kopaonik domes starting at around 21–17 Ma as indicated by ^{40}Ar/^{39}Ar ages on biotite (Schefer 2010) and ending around 10 Ma (AFT and ZFT data — Schefer et al. 2011). The tectonic omission was

Table 1: Locality and lithology of the samples. **VR** — vitrinite reflectance, **AFT** — apatite fission track, **ZFT** — zircon fission track.

Sample	Local coordinates (MGI Balkans 7) (m)	Latitude–longitude (decimal degrees)	Altitude (m)	Depth (m)	Lithology	Location	Method of investigation
IBM-1/1			409.50	43.5–44.5	Shale		VR
IBM-1/2			406.10	47.0–47.9	Shale		VR
IBM-1/3			387.20	63.2–66.8	Shale		VR
IBM-1/4			330.10	122.8–123.9	Shale		VR
IBM-1/6			325.80	127.0–128.2	Shale		VR
IBM-1/7			257.40	195.4–196.6	Shale		VR
IBM-1/8			226.40	226.3–227.6	Shale		VR
IBM-1/23	7472377.63	N 43.38174	147.40	302.5–306.6	Sandstone		AFT, ZFT
IBM-1/24	4804201.05	E 20.65376	134.30	318.3–319.7	Sandstone		AFT, ZFT
IBM-1/25			110.30	342.1–343.7	Conglomerate		AFT, ZFT
IBM-1/27			109.50	344.2–344.5	Shale	Piskanja deposit	VR
IBM-1/28			101.80	344.5–352.2	Sandstone		AFT, ZFT
IBM-1/29			100.80	352.2–353.2	Shale		VR
IBM-1/30			79.70	373.5–374.3	Sandstone		AFT, ZFT
IBM-1/31			72.00	381.9–382.0	Coal fragments in shale		VR
IBM-1/22			46.80	409.3–409.5	Conglomerate		AFT, ZFT
IBM-2/15			114.53	318.5–320.1	Sandstone		AFT, ZFT
IBM-2/17	7472179.85	N 43.38207	74.98	359.05–359.95	Sandstone		AFT, ZFT
IBM-2/19	4804237.84	E 20.65132	53.73	379.4–381.2	Sandstone		AFT, ZFT
IBM-2/21			39.73	394.7–395.2	Shale		VR
IBM-4/41	7471435.92	N 43.37865	250.46	149.4–152.3	Sandstone		AFT, ZFT
IBM-4/44	4803862.07	E 20.64216	90.06	309.1–312.7	Sandstone		AFT, ZFT
Tadenje 11			457.40	47.6–48.6	Coal		VR
Tadenje 12			457.20	48.6–48.8	Sandstone		AFT, ZFT
Tadenje 14			455.70	49.6–50.3	Coal		VR
Tadenje 15	7469179	N 43.43155	437.60	68.2–68.4	Sandstone	Tadenje underground coal mine	AFT, ZFT
Tadenje 1	4809748	E 20.61397	437.40	68.4–68.6	Coal		VR
Tadenje 13			436.40	69.5–69.6	Sandstone		AFT, ZFT
Tadenje 10A			435.30	70.5–70.7	Coal		VR
Tadenje 10B			435.00	70.7–71.0	Coal		VR
1-Biljanovac	7472085 4807161	N 43.40837 E 20.65000	383.00	Surface	Volcanoclastite	Biljanovac	AFT, ZFT
8-Pruga	7471207 4802855	N 43.36958 E 20.63938	399.00	Surface	Andesite/ volcanoclastite	Pruga	AFT, ZFT
4-Kremići	7477304 4800615	N 43.34963 E 20.71471	1140.00	Surface	Granodiorite	Kremići	AFT, ZFT
9-Kremići	7474777 4800961	N 43.35266 E 20.68352	808.00	Surface	Hydrothermally altered andesite		AFT, ZFT
3-Drenje	7483607 4806320	N 43.40115 E 20.79228	740.00	Surface	Granodiorite	Drenje	AFT, ZFT

about 10 km (Schefer 2010). The core-complex formation was coeval with the emplacement of the S-type Polumir granite (18.1–17.4 Ma), Golija granite (20.6–20.2 Ma) and exhumation of the older Oligocene I-granitic rocks of Kopaonik and Drenje (Schefer et al. 2011). The Miocene volcanic activity is represented by effusives and pyroclastites of quartz-latitic composition. The Miocene volcanics occur south-west of the Kopaonik intrusives and in the surroundings of the Golija pluton (Cvetković & Pécskay 1999; Cvetković 2002).

The Ibar Basin was formed in the hanging wall of the Studenica core-complex, but it also possibly records a brittle phase (mainly E-W directed, and subordinately N-S) of exhumation of the Kopaonik Metamorphic Series (Schefer 2010). Deposition started with continental alluvial, syn-kinematic breccio-conglomerates, sandstones and marlstones intercalated with up to nine bituminous coal seams (Anđelković et al. 1991; Ercegovac et al. 1991). This succession is overlain by laminated dolomitic marlstones and claystones, deposited in a lacustrine environment. The overall present day thickness of the sediments deposited in the Ibar Basin is around 1500 m (based on geophysical exploration — Anđelković et al. 1991). The basin is characterized by the presence of bituminous coals (%Rr up to 0.91 — Ercegovac et al. 1991), boron mineralization (borates and howlite — Obradović et al. 1992), magnesite deposits (Falick et al. 1991) and travertine (noticed during field observation). Other intramontane coal basins in Serbia, which cover the same stratigraphic range, did not exceed the subbituminous stage of coalification (%Rr ~ 0.45 — Ercegovac et al. 2006; Životić et al. 2008, 2010). The relatively high rank of Cenozoic coals from the Ibar Basin according to Ercegovac et al. (1991) is due to the thermal influence of andesitic extrusion.

The age of sediments is not well constrained. According to correlation of sediments from other intra-montane basins in the Dinaridic lake system it could be inferred that alluvial deposition started around 19–17 Ma (Prysjazhnjuk et al. 2000; Krstić et al. 2001) and lasted until 16–15 Ma when a typical lacustrine environment was established (Kochansky & Slisković 1981). Combining geodynamic (Schefer 2010) and paleontological lines of evidence (Prysjazhnjuk et al. 2000; Krstić et al. 2001) in the following discussion we adopt 19 Ma as the age of the onset of sedimentation in the Ibar Basin. Today the Ibar Basin can be characterized as a composite basin which is formed by four sub-basins (Fig. 1): Tadenje, Ušće, Jarando, and Gradac (Ercegovac et al. 1991). The sediments studied here from the Piskanja deposits represent the south-eastern part of the Jarando sub-basin.

Sampling strategy and analytical methods

The thermal history of the Ibar Basin has been studied by means of vitrinite reflectance and detritial apatite and zircon fission track data targeting the maximum paleotemperatures and duration of the thermal event, cooling manner (slow/fast) from maximal paleotemperatures, respectively.

The majority of samples were collected from boreholes in the Piskanja deposit and Tadenje underground coal mine.

Vitrinite reflectance was measured on dispersed organic matter on eleven shale samples (seven are positioned in lacustrine and four in alluvial facies; Table 1) from the Piskanja deposit and five coal samples from the Tadenje underground coal mine (Tadenje sub-basin).

For the fission track analysis fifteen core samples (conglomerate and sandstone) from three boreholes (IBM-1, IBM-2, and IBM-4) in the Piskanja deposit, and three channel sandstone samples between coal layers in the Tadenje sub-basin were collected (Table 1, Fig. 2). Five samples of andesite, hydrothermally altered andesite, granodiorite and volcanoclastic rocks, were taken from outcrops in the surrounding area in order to study the tectono-thermal history (cooling and exhumation) of the basin margin and its relation to basin fill.

The detrital apatite and zircon may be derived from diverse sources, meaning that they carry information about the thermal history of the sediment's provenance regions. After deposition the thermal history of the sediments can follow at least three possible scenarios: i) experienced temperatures were not high enough (above the partial annealing zone (PAZ, 60 °C–120 °C) to cause annealing of the fission track so that all the AFT single ages will be equal/slightly younger or older than the depositional age; ii) experienced temperatures were higher than PAZ for ~10^7 Ma to cause total resetting of the AFT single ages so that all the AFT single ages are younger than the depositional age and iii) experienced temperatures were in the range of the PAZ for a shorter period of time > 10^7 Ma producing partially annealed grains with AFT single ages older and younger than the age of deposition (Gleadow et al. 1986; Laslett et al. 1987; Wagner & van den Haute 1992).

Vitrinite reflectance (VR)

For rank determination, the laminated dolomitic marl samples were cut, mounted in epoxy resin and polished, while coal samples were crushed to a maximum particle size of

Table 2: Vitrinite reflectance data and estimated paleotemperatures. [a]**Tpeak** = (ln (VRr) + 1.68)/0.0124, burial heating (Barker & Pawlewicz 1986), **±0.10** — standard deviation, **(n=50)** — number of measurements.

Sample	Depth (m)	Average vitrinite reflectance %Rr	Estimated paleotemperature (°C)
IBM-1/1	43.5–44.5	0.66±0.10 (n=50)	102[a]
IBM-1/2	47.0–47.9	0.68±0.11 (n=50)	104[a]
IBM-1/3	63.2–66.8	0.71±0.08 (n=50)	108[a]
IBM-1/4	122.8–123.9	0.76±0.09 (n=50)	113[a]
IBM-1/6	127.0–128.2	0.69±0.09 (n=50)	106[a]
IBM-1/7	195.4–196.6	0.77±0.09 (n=50)	114[a]
IBM-1/8	226.3–227.6	0.77±0.09 (n=50)	114[a]
IBM-1/27	344.2–344.5	0.76±0.09 (n=50)	113[a]
IBM-1/29	352.2–353.2	0.74±0.08 (n=50)	111[a]
IBM-1/31	381.9–382.0	0.69±0.07 (n=50)	106[a]
IBM-2/21	394.7–395.2	0.63±0.06 (n=50)	98[a]
Tadenje 11	47.6–48.6	0.87±0.03 (n=50)	125[a]
Tadenje 14	49.6–50.3	0.86±0.03 (n=50)	124[a]
Tadenje 1	68.4–68.6	0.90±0.02 (n=50)	127[a]
Tadenje 10A	70.5–70.7	0.90±0.03 (n=50)	127[a]
Tadenje 10B	70.7–71.0	0.90±0.03 (n=50)	127[a]

Table 3: Fission track results from the Ibar Basin. **Ap** — apatite, **Zr** — zircon, **N** — number of counted grains per sample, **ρd (Nd)** — density of dosimeter tracks (number of counted dosimeter tracks), **ρs (Ns)** — density of spontaneous tracks (number of counted spontaneous tracks), **ρi (Ni)** — density of induced tracks (number of counted induced tracks), **P(χ²)** — is the probability of obtaining χ² values for n degrees of freedom where n=number of crystals-1. Central age ±1σ (Ma) (Galbraith & Laslett 1993), **MTL ±1σ (μm)** — mean track length, **SD (μm) (N)** — standard deviation (number of horizontal confined tracks measured), **Dpar (μm)** — mean track pit length, **U conc.** — concentration of U in ppm.

Sample	Lithology	Mineral	N	ρd (Nd) x10⁶cm²	ρs (Ns) x10⁶cm²	ρi (Ni) x10⁶cm²	P(χ²) (%)	U conc. (ppm)	Central ±1σ (Ma)	MTL ±1σ (μm)	SD (μm) (N)	Dpar (μm)
IBM-1/22	Sandstone	Ap	12	1.296 (4436)	0.149 (44)	1.398 (411)	85.25	12±8	22.9±4.0			
IBM-1/23	Sandstone	Ap	12	1.326 (5017)	0.309 (248)	2.486 (1992)	0.22	22±6	26.4±3.5			
		Zr	21	0.39 (4122)	2.416 (1276)	2.405 (1270)	73.66	194±56	28.7±2.8			3.3
IBM-1/24	Sandstone	Ap	25	1.446 (5017)	0.288 (618)	2.799 (5988)	0.21	22±7	25.1±2.3	11.26±2.61	2.53 (17)	
		Zr	22	0.422 (4108)	3.556 (1655)	3.720 (1731)	99.32	300±111	29.1±2.8			
IBM-1/25	Conglomerate	Ap	15	1.261 (4436)	0.304 (407)	2.288 (3062)	0.06	20±7	25.6±3.3	12.32±2.23	2.19 (35)	2.4
IBM-1/28	Sandstone	Ap	19	1.227 (4436)	0.238 (255)	2.011 (2151)	1.89	18±10	26.0±2.9	10.63±2.36	2.34 (67)	2.4
IBM-1/30	Sandstone	Ap	17	1.314 (4436)	0.124 (184)	1.237 (1834)	51.75	11±5	21.5±2.2	10.82±2.52	2.47 (24)	2.3
IBM-2/15	Sandstone	Ap	17	1.390 (5017)	0.289 (590)	2.193 (5017)	28.02	17±6	30.4±2.5	11.43±2.10	2.08 (49)	2.7
		Zr	21	0.398 (4122)	2.412 (1480)	2.195 (1347)	80.65	185±79	31.5±3.1			
IBM-2/17	Sandstone	Ap	20	1.300 (4436)	0.167 (239)	1.292 (1843)	30.40	12±6	27.8±2.8	10.35±2.21	2.03 (13)	2.6
IBM-2/19	Sandstone	Ap	15	1.435 (4436)	0.136 (198)	1.316 (1912)	13.91	12±5	24.8±2.8	11.21±2.94	2.90 (32)	2.4
IBM-4/41	Sandstone	Ap	22	1.400 (5017)	0.349 (1089)	2.906 (9044)	0.41	24±7	28.0±2.3	10.98±2.39	2.38 (102)	2.8
		Zr	20	0.429 (4108)	3.631 (1217)	3.891 (1304)	98.71	295±85	28.8±2.9			
IBM-4/44	Sandstone	Ap	20	1.526 (5017)	0.370 (2129)	3.114 (2129)	18.94	26±13	29.6±3.0	10.11±1.97	1.92 (21)	2.7
		Zr	23	0.403 (4108)	3.477 (938)	3.542 (957)	99.41	290±110	28.5±2.9			
Tadenje 12	Sandstone	Ap	25	1.398 (5017)	0.264 (297)	3.084 (3467)	19.40	25±6	18.0±1.8	11.44±2.59	2.56 (46)	2.4
		Zr	23	0.426 (4108)	5.655 (934)	8.416 (1390)	25.57	625±167	20.6±2.1			
Tadenje 13	Sandstone	Zr	27	0.394 (4122)	4.679 (1664)	7.402 (2632)	31.13	608±109	18.0±1.7			
Tadenje 15	Sandstone	Ap	32	1.592 (4436)	0.124 (494)	1.974 (7869)	34.17	17±5	16.5±1.4	9.90±2.45	2.45 (63)	1.8
1-Biljanovac	Volcanoclastite	Ap	30	1.500 (5017)	0.329 (902)	4.485 (12286)	7.13	35±13	18.3±1.5	13.21±1.73	1.70 (29)	2.8
		Zr	18	0.399 (4122)	0.801 (796)	1.185 (1177)	2.22	99±30	19.2±2.1			
8-Pruga	Andesite/ volcanoclastite	Ap	20	1.518 (5017)	0.253 (351)	3.833 (5315)	80.97	30±7	16.4±1.5	12.19±2.51	2.43 (15)	2.6
		Zr	20	0.395 (4122)	1.390 (1513)	1.611 (1754)	63.10	220±65	25.3±2.5			
9-Kremići	Hydrothermally altered andesite	Ap	25	1.311 (5017)	0.257 (666)	3.725 (9653)	1.75	33±11	15.3±1.3			
		Zr	23	0.385 (4122)	2.115 (2040)	2.628 (2535)	1.06	344±79	22.5±2.2			
4-Kremići	Granodiorite	Ap	23	1.400 (5017)	0.266 (580)	3.638 (7932)	15.81	31±12	17.1±1.4	14.21±1.05	1.50 (99)	2.8
		Zr	23	0.424 (4108)	1.536 (436)	2.631 (747)	63.99	204±63	17.8±1.9			
3-Drenje	Granodiorite	Ap	24	1.487 (4436)	0.203 (212)	3.409 (3558)	96.99	26±11	14.7±1.5	11.33±1.97	1.95 (47)	1.7

1 mm, mounted in epoxy resin and polished. The reflectance measurements were performed under a monochromatic light of 546 nm using a Leitz MPV microscope and optical standards having a reflectance of 0.8999 % and 1.6999 % in oil, following the procedures outlined by Taylor et al. (1998). The rank was determined by measuring the random reflectance on colotelinite B. The reflectance measurements were performed at the Department für Angewandte Geowissenschaften und Geophysik, Montanuniversität Leoben.

During burial diagenesis of organic matter, the optical reflectivity of vitrinite increases as a result of increasing temperatures. As vitrinite reflectance is not susceptible to retrograde alteration, it may be considered a geothermometer for maximum paleotemperatures. According to different kinetic models and field studies, vitrinite reflectance may be used with caution to estimate absolute maximum paleotemperatures, as shown by Barker & Pawlewicz (1986). They published different vitrinite reflectance temperature correlations for long-term (burial) and short-term (hydrothermal) heating. Maximum paleotemperatures were calculated according to the methodology explained in Barker & Pawlewicz (1986) for burial heating, and the results are given in Table 2.

Apatite and zircon fission track analysis

The samples were mounted in epoxy resin (apatite) and PFA Teflon (zircon) after conventional mineral separation (crushing, sieving, magnetic, and heavy liquid separation) at the University of Belgrade and partly at the University of Innsbruck. Etching of apatite mounts were done in 6.5% HNO_3 at 20 °C for 40 s. Zircon mounts were etched in a NaOH–KOH eutectic melt for 4–8 h at 235 °C. Induced tracks in external detector muscovite were etched in 40% HF for 45 min at 20 °C. Irradiation was carried out at FRMII Garching (Technische Universität München, Germany). Neutron flux was monitored using CN5 and CN1 dosimeter glasses for apatite and zircon, respectively. Densities of spontaneous, induced tracks and for the apatites confined horizontal lengths and Dpar measurements were performed on a Zeiss Axioplan microscope equipped with Autoscan®, System at 1250× magnification, dry objective at the University of Innsbruck. All samples have been analysed using an external detector (Gleadow 1981). The fission-track central ages were determined using zeta approach (Hurford & Green 1983) with zeta factors of 330±9.45 for the apatite (CN5 dosimeter glass) and 144±12.89 for the zircon, (CN1 dosimeter glass) (analyst Nevena Andrić). The AFT and ZFT central ages are reported with 1σ error (Galbraith & Laslett 1993). The TRACKKEY program, version 4 was used in data processing (Dunkl 2002). The homogeneity of the age population was determined by Chi (χ^2) test (Gleadow et al. 1986; Galbraith & Laslett 1993). The Dpar method (Donelick 1993; Burtner et al. 1994) was used as a proxy for annealing properties. For identification of different age components or peak ages for the samples with spread ages, the binomial peak-fitting method was used (Galbraith & Green 1990; Brandon 2002).

The analytical results are given in Table 3 and location of the samples in Fig. 2. Due to the quality of the apatite and zircon grains it was not possible to obtain the age pairs (AFT
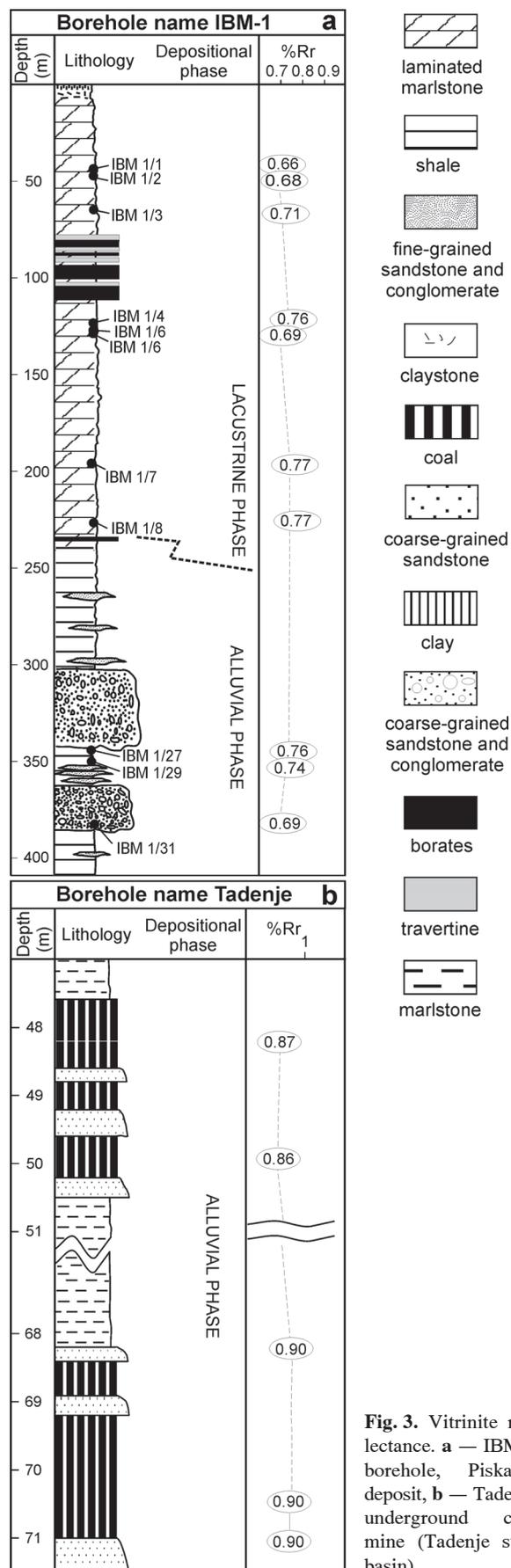

Fig. 3. Vitrinite reflectance. **a** — IBM-1 borehole, Piskanja deposit, **b** — Tadenje underground coal mine (Tadenje subbasin).

and ZFT) for each sample. Modelling of the apatite age and track-length distribution data was carried out with the program HeFTy (Ketcham et al. 2003). The input parameters were AFT age data, track length distributions and etch pit diameters (Dpar). Time-temperature boxes were defined by additional input constraints for the model, namely: ZFT and AFT central, single ages and geological constraints. The partial annealing zone (PAZ) of apatite is constrained between 120 °C and 60 °C (Laslett et al. 1987) and of zircon ~200 °C and 320 °C (Tagami et al. 1998). The present day temperature on the surface was set to 20 °C. The generation of time-temperature paths was done using the inverse Monte Carlo algorithm (Ketcham 2005). The c-axis projections were corrected using the annealing model of Ketcham et al. (2007). The modelling results were statistically evaluated by the goodness of fit (GOF) of measured and modelled data. The value >0.5 between modelled and measured data was considered a "good" fit, while a value of 0.05 or higher was "acceptable".

Results

Vitrinite reflectance data

The vitrinite reflectance results vary from 0.63 to 0.90 %Rr (Table 2) implying a bituminous stage of organic matter. In the boreholes IBM-1 and IBM-2 (Piskanja deposit) the vitrin-ite reflectance values do not show a pronounced depth trend. The data are spread between 0.63 % and 0.77 %Rr, whereas most values are overlapping within one standard deviation (0.11–0.07 %; Table 2, Fig. 3). The vitrinite reflectance in coal seams from the Tadenje sub-basin (northern part of the basin) increases from 0.86 % at 47.60 m to 0.90 %Rr at 71.00 m. Typical coalification temperatures for the bituminous coals with such vitrinite reflectance values are approximately 100–130 °C (Barker & Pawlewicz 1986). The higher values in the Tadenje sub-basin indicate higher maximum paleotemperatures than in the Piskanja deposit.

Zircon and apatite fission track data

The samples in the Piskanja deposit yielded ZFT central ages from 28.7±2.8 Ma to 31.5±3.1 Ma (Table 3, Fig. 4a). All samples pass the χ^2 test indicating single grain age population of zircons (P (χ^2) >5 %, Galbraith 1981). The AFT central ages range between 21.5±2.2 Ma and 30.4±2.5 Ma, whereas single grain ages range from 6.7 Ma to 45.0 Ma (Table 3, Fig. 5). The mean track length varies from 12.32±2.23 μm to 10.11±1.97 μm (Table 3, Fig. 6). The samples IBM-1/22, IBM-1/30, IBM-2/15, IBM-2/17, IBM-2/19, and IBM-4/44 contain one apatite single grain age population, meaning that they pass the χ^2 test (P (χ^2) >5 % — Galbraith 1981). The samples IBM-1/23, IBM-1/24, IBM-1/25, IBM-1/28 and IBM-4/41 failed the χ^2 test (P (χ^2) <5% — Galbraith
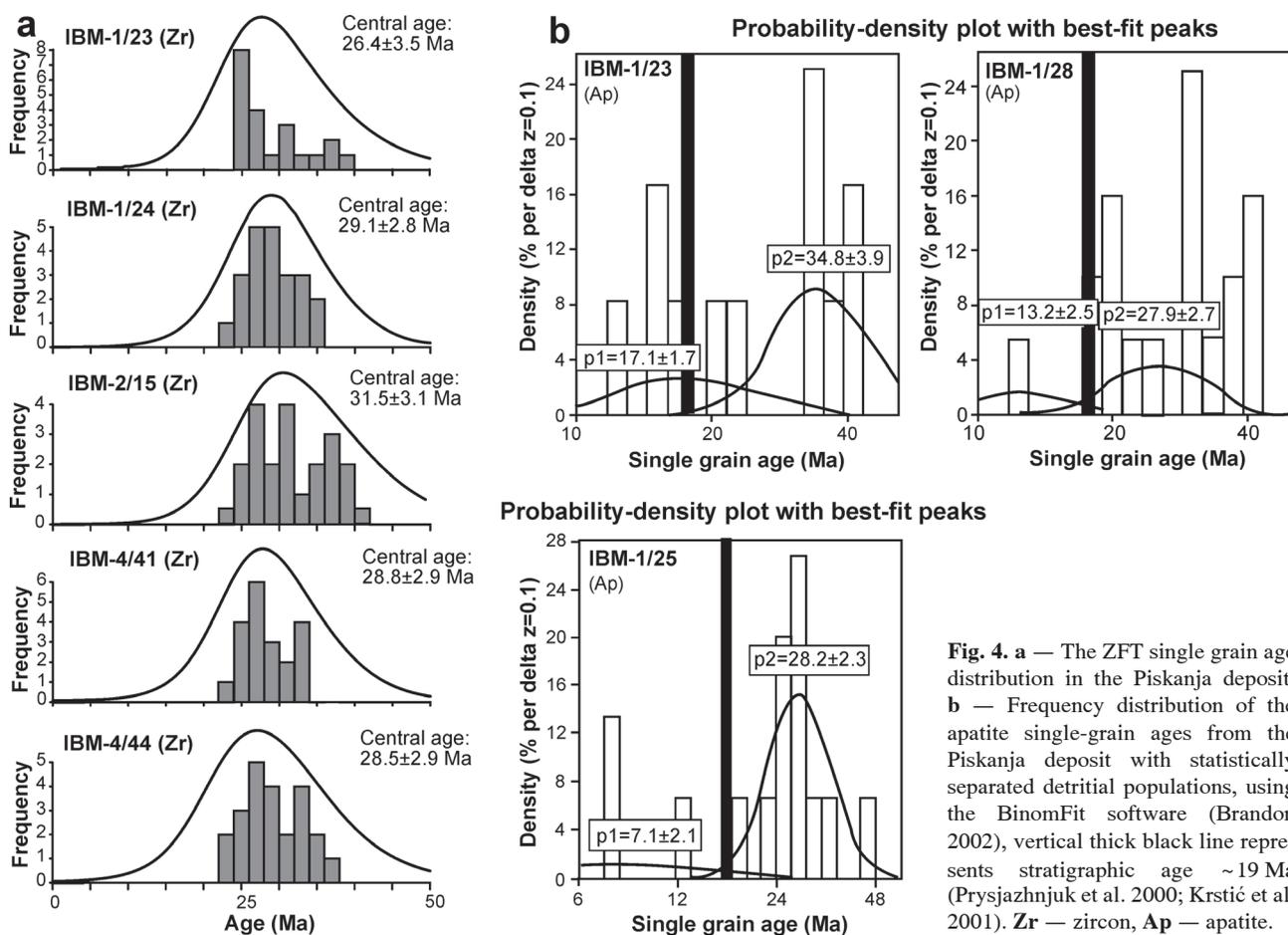

Fig. 4. a — The ZFT single grain age distribution in the Piskanja deposit, **b** — Frequency distribution of the apatite single-grain ages from the Piskanja deposit with statistically separated detritial populations, using the BinomFit software (Brandon 2002), vertical thick black line represents stratigraphic age ~19 Ma (Prysjazhnjuk et al. 2000; Krstić et al. 2001). **Zr** — zircon, **Ap** — apatite.
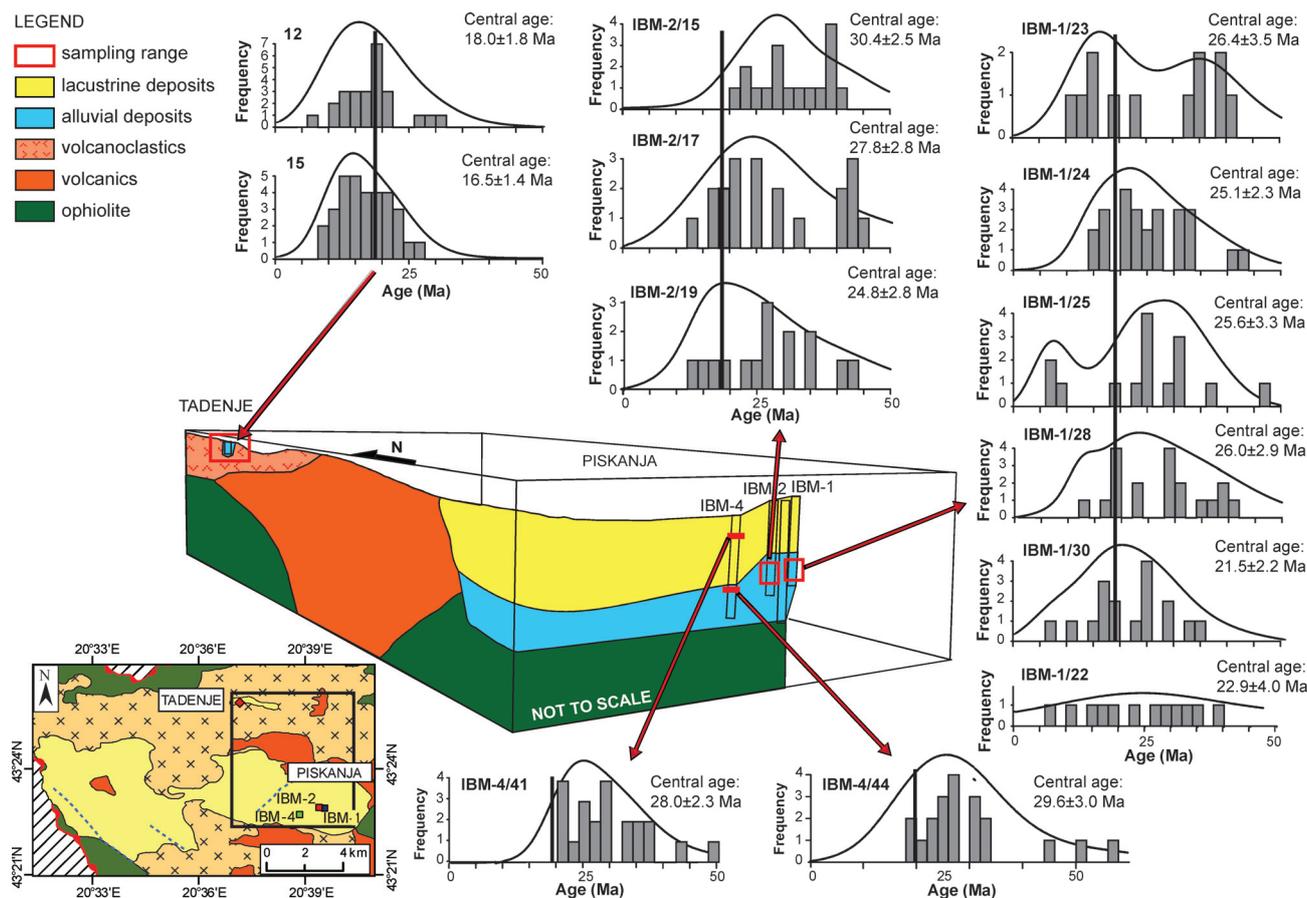
Fig. 5. The AFT single grain age distribution in Piskanja and Tadenje deposit. Vertical thick black line represents stratigraphic age ~ 19 Ma (Prysjazhnjuk et al. 2000; Krstić et al. 2001).

1981), suggesting more than one single grain age population. Samples IBM-1/23, IBM-1/25, IBM-1/28, and IBM-1/30 contain two subpopulations, statistically separated (Fig. 4b). The first subpopulation comprises peaks at 17.1 ± 1.7 Ma (IBM-1/23), 7.1 ± 2.1 Ma (IBM-1/25) and 13.2 ± 2.5 Ma (IBM-1/28) which are younger than the age of deposition (Fig. 4b). The second subpopulation is characterized by peaks older than the age of deposition, 34.8 ± 2.3 Ma (IBM-1/23), 28.2 ± 2.3 Ma (IBM-1/25) and 27.9 ± 2.7 Ma (IBM-1/28).

In the Tadenje sub-basin the ZFT central ages are 18.0 ± 1.7 Ma and 20.0 ± 2.1 Ma (Table 3, Fig. 6). The AFT central ages are 16.6 ± 1.4 Ma and 19.9 ± 2.0 Ma (Fig. 5) with mean track lengths of 9.90 ± 2.45 μm and 11.44 ± 2.59 μm. All samples (apatite and zircon) pass the χ^2 test, indicating that all single grains belong to the same population (P (χ^2) >5% — Galbraith 1981). Thermal modelling of these samples (Tadenje 12 and Tadenje 15) revealed post-depositional heating with maximum temperatures around 100 °C (Fig. 8). The heating lasted from 18–17 to 10–8 Ma. Cooling started at about 10–8 Ma and reached the present-day temperature of 28 °C at a depth of 70 m.

The ZFT central ages of the outcropping magmatic rock in the basin margin range from 17.8 ± 1.9 Ma to 25.3 ± 2.5 Ma (Table 3). The AFT central ages range between 15.3 ± 1.3 Ma and 18.2 ± 1.6 Ma (Table 3). The samples have mean track length between 12.19 ± 2.51 μm and 14.21 ± 1.05 μm. With

the exception of 9-Kremići, all samples pass the χ^2 test indicating a homogenous population (P (χ^2) >5 % — Galbraith 1981). The fission track analysis of the Biljanovac volcanoclastites gave similar zircon and apatite ages, of 19.2 ± 2.1 Ma and 18.4 ± 1.5 Ma, respectively and relatively long mean track length, 13.21 ± 1.73 μm (Table 3, Figs. 6, 7). Thermal modelling reveals that 1-Biljanovac sample underwent fast cooling through both zircon and apatite PAZ, from 20 Ma to 18 Ma (Fig. 8). The cooling history of sample 4-Kremići indicated rapid cooling from above ZPAZ, namely 300 °C to around 80 °C (20–17 Ma), followed by slower cooling to the surface temperatures (Fig. 8). This scenario is reflected in identical zircon and apatite ages (17.8 ± 1.9 Ma and 17.1 ± 1.4 Ma) and long mean track length (14.21 ± 1.05 μm).

Discussion

Compilation of new VR, AFT, ZFT data and literature data enabled reconstruction of the Ibar basin's evolution, emphasizing its thermal history. The low temperature thermochronology and new vitrinite reflectance data on the Miocene syn-kinematic sediments of the Ibar supradetachment basin documented post-depositional thermal overprint and proposed mechanism that controlled the thermal state of the basin. The correlation between AFT and ZFT ages of basement
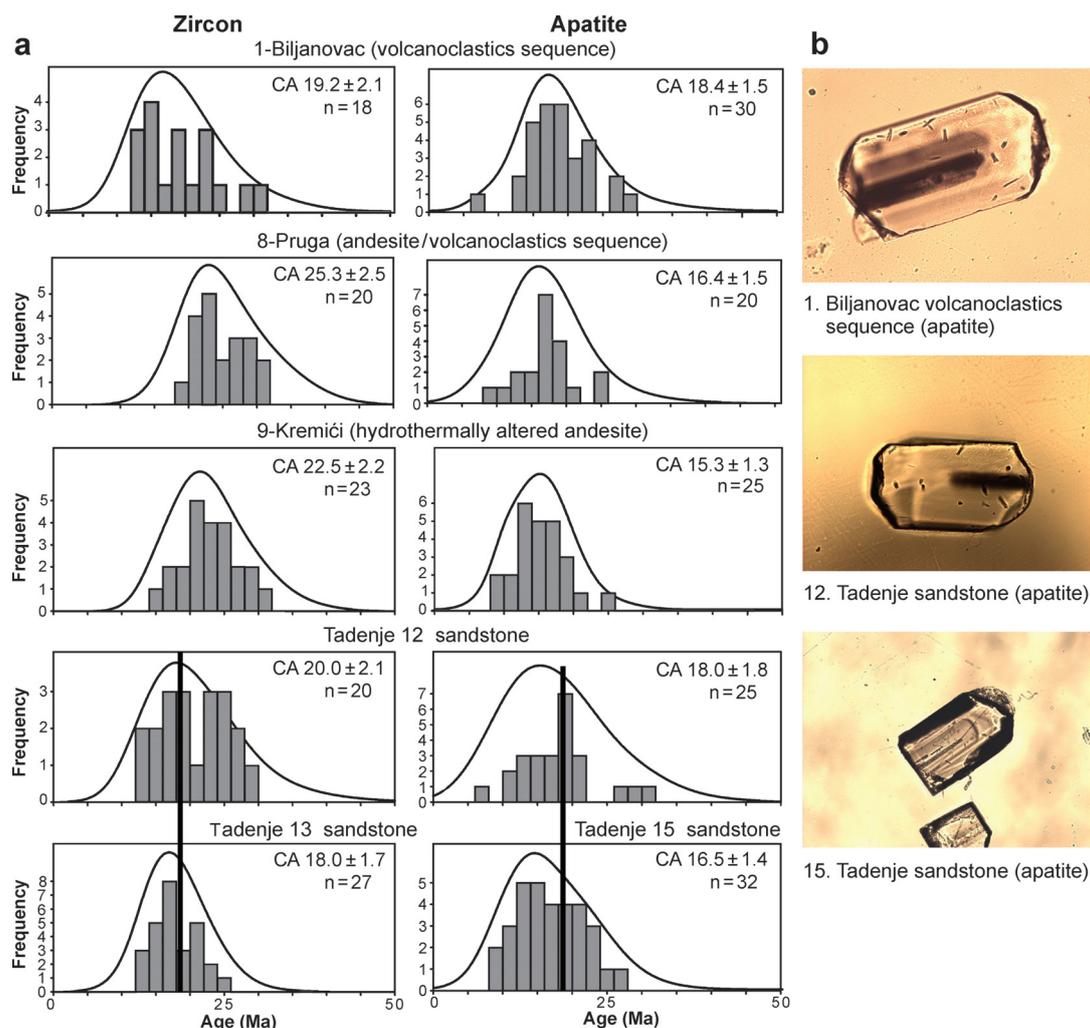
Fig. 6. a — Single grain age distribution of zircon (**zr**) and apatite (**ap**) in selected samples. Vertical thick black line represents stratigraphic age ~19 Ma (Prysjazhnjuk et al. 2000; Krstić et al. 2001), **b** — Apatite morphology in samples 1-Biljanovac, Tadenje 12 and Tadenje 15.

rocks and ages of basin fill indicated synchronous basement (source area) exhumation and deposition in the basin.

The ZFT central ages of the sediments from Ibar Basin are similar to the depositional age (Table 3). This means that the zircons have preserved the information about the cooling history of the source region from where they were eroded (Hurford & Carter 1991; Wagner & van den Haute 1992). The presence of andesitic fragments in conglomerates and sandstones from Piskanja, together with ZFT age distribution suggests Oligocene andesite as one of the dominant sediment sources (Figs. 5, 6, 7). In the Tadenje sub-basin ZFT single age spectra in the sandstones correspond to the age spectra of outcropping volcanoclastites (1-Biljanovac, Fig. 6a). The andesites and their volcanoclastic counterparts formed the paleorelief in this part of the basin, which furthermore implies that these rocks were most probably the source for sediments. This is further supported by the presence of apatite grains with subhedral shape and black inclusions (Fig. 6b), which are observed only in the 1-Biljanovac volcanoclastite and sandstones from the Tadenje sub-basin. The close ages between the detrital grains and age of depo-

sition suggest fast exhumation of the basement source rocks during the Early Miocene and synchronous erosion and sedimentation. The thermal modelling of the 4-Kremići granodiorite sample supports that conclusion (Fig. 8).

In the Ibar Basin AFT central ages are older (Piskanja) or slightly younger (Tadenje) than the age of deposition (Fig. 5). The apatite single grain age spectra of the studied sediments showed spread AFT single grain ages with a significant number of grains, which are younger than the age of deposition (Fig. 5). This implies that the apatites in the sediments are partially annealed (Green et al. 1986; Laslett et al. 1987; Wagner & van den Haute 1992) due to post-depositional thermal overprint supported by vitrinite reflectance data. Although the apatites were exposed to maximum paleotemperatures of ~120 °C (vitrinite reflectance data), the detritial apatites still contain older age components and broad track length distribution as evidence of partial resetting (Figs. 5, 6, 7). This implies that the apatites must have experienced elevated temperatures for a relatively short time, given that after 10 Ma at such temperatures total annealing of fission tracks in apatites should have occurred (Laslett et al. 1987).
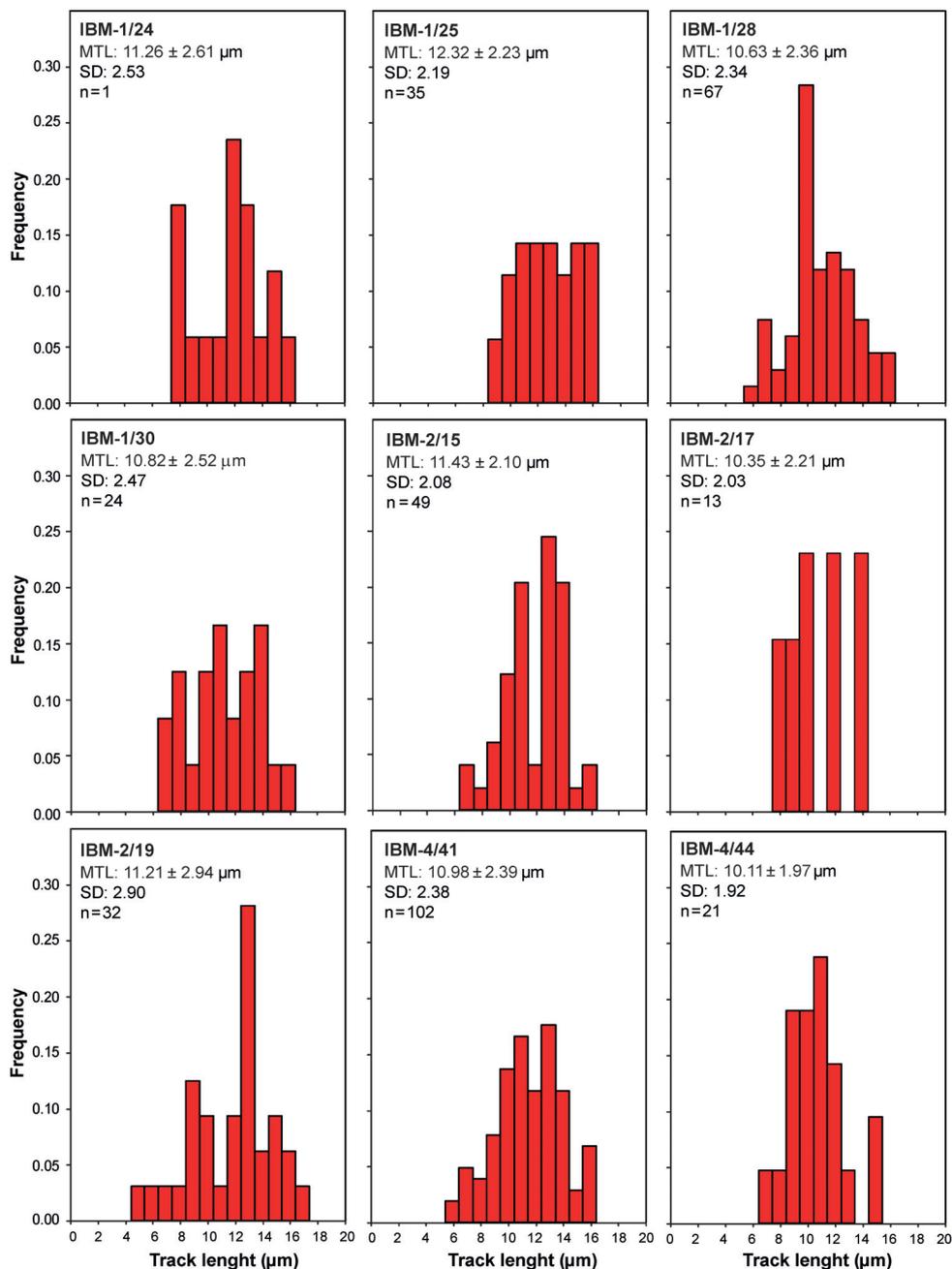
Fig. 7. Apatite fission track length distribution in the studied sediments. **MTL** — mean track length, **SD** — standard deviation, **n** — number of tracks.

The thermal modelling supports this conclusion that the apatites were annealed between 17 Ma and 10–8 Ma (Fig. 8).

In the Piskanja deposit the evidence of the post-depositional thermal overprint (~100–120 °C, vitrinite reflectance; Table 2) is noticed only in the AFT samples from borehole IBM-1 and from the deepest parts of IBM-2 (IBM-2/17, IBM-2/19). The samples from IBM-4 and IBM-2/15 holes seem to be unaffected by the thermal overprint. The thermal overprint intensity in the boreholes decreases laterally from IBM-1 to IBM-4 and this implies decreasing temperatures towards the basin center. That could, tentatively, suggest this thermal overprint was more local influencing only the mar-

gin of the Piskanja deposit. Again tentatively, the time frame of this thermal perturbation could be inferred from the youngest AFT peak age subpopulation in the borehole IBM-1, ~7.1 Ma (Fig. 4b).

In the Tadenje sub-basin, the current overburden of 70 m is very much less than that required to explain the deduced paleotemperatures (120–130 °C, Table 2) and significant annealing of the apatites in the sediments (Fig. 5). In the case of the present day average geothermal gradient (~25–30 °C/km — Milojević 1993; Lenkey et al. 2002) the expected overburden necessary for such paleotemperatures is between 4 and 5 km. This overburden should be considered as a maxi-
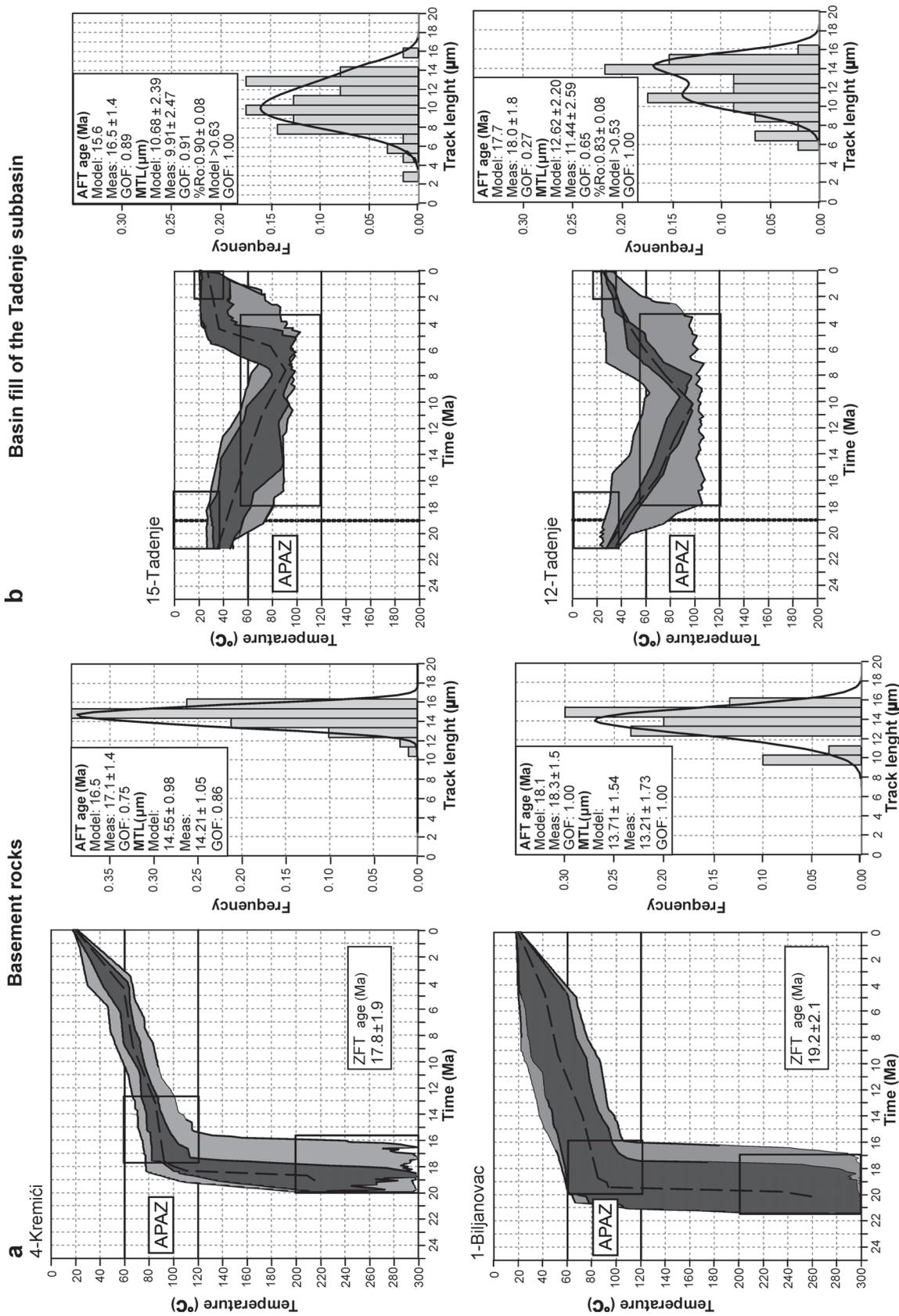
Fig. 8. a — Modelled thermal history of basement rocks (Kremići granitoid and Biljanovac volcanoclastics). The black boxes represents modelling constraints, ZFT and AFT ages including their 1 σ errors within zircon (~200 °C and 320 °C — Tagami et al. 1998) and apatite (between 60 °C and 120 °C — Laslett et al. 1987) partial annealing zone, **b** — Modelled thermal histories of detrital AFT data in the Tadenje deposit. The starting T-t boxes are established by the onset of deposition 19±2 Ma, when the samples were forced to be on the surface and (partially) annealed AFT single grain ages including their 1 σ errors when samples were within the APAZ. **APAZ** — apatite partial annealing zone. The light grey envelopes represent acceptable and the dark grey ones good fits between modelled and measured data. Vertical thick black line represents stratigraphic age ~ 19 Ma (Prysjazhnjuk et al. 2000; Krstić et al. 2001).

mum estimate, based on assumed higher geothermal gradients due to intense magmatic activity during the Miocene in this region.

The formation of the Ibar Basin is related to the exhumation of the Studenica and Kopaonik core-complexes during the Early Miocene (from 21–17 Ma to 10 Ma — Schefer 2010). This stage was characterized by rapid decompression and by normal-shearing within the detachment evident by syn-deformational emplacement of the Polumir granitoid (Schefer 2010). In the same period (~19 Ma) the hanging wall subsided along the detachment creating accommodation space for the basin fill.

The provenance ZFT ages in the studied sediments suggest contemporaneous fast exhumation, erosion and sedimentation. The deposition was followed by heating from around 17 Ma reaching the maximal paleotemperatures of ~120–130 °C around 10–8 Ma when subsequent cooling to the present day temperatures started (Fig. 8). This heating phase is contemporaneous with the juxtaposition of the warmer lower crustal rocks (Studenica and Kopaonik metamorphic domes) with the upper crust (including the Ibar Basin). The thermal evolution of the footwall, based on t-T paths of the Kremići (this study), Kopaonik, Željin, Drenje, and Polumir plutons (Schefer et al. 2011), indicates continuous rapid cooling between ~16 and 10 Ma from ~300 °C to 60 °C (Fig. 8; 4-Kremići sample). Along the contact between warm footwall and cold hanging wall thermal gradient is the highest, enabling heat transfer by conduction affecting the basin fill (Souche et al. 2012).

Higher vitrinite reflectance values and a higher degree of partial resetting in apatites in the Tadenje sub-basin compared to the Piskanja deposit could be the result of a different primary stratigraphic position of the samples. On the other hand, gradual exhumation of the metamorphic dome can create an asymmetry of temperatures in the basin which increases towards the detachment (Souche et al. 2012). This temperature asymmetry can produce differences in thermal overprint within the basin. The cooling in the basin after 10–8 Ma is probably related to the basin's inversion and erosion. The more local heat source which only affected the Piskanja deposit, mostly along its margin, could be additionally attributed to nearby magmatic and/or hydrothermal activity, the effects of which are seen from stratabound mineralizations of boron, magnesite and travertine. The inferred time for this activity perfectly overlaps with the youngest phase of high-K calc-alkaline to shoshonitic and ultrapotassic volcanic activity in Serbia (Cvetković et al. 2004).

Conclusion

The result of vitrinite reflectance and apatite fission track data helped to quantify the thermal overprint of the Ibar Basin, reaching the maximum paleotemperatures of around 120–130 °C. The higher values of vitrinite reflectance in the Tadenje sub-basin indicate higher maximum paleo-temperatures than in the Piskanja deposit. The modelled thermal history of the detrital apatites indicates heating episode from around 17 Ma ago to around 10–8 Ma when cooling began.

In the Piskanja deposit (southeastern part of the Ibar Basin) a local heat source may have caused an additional thermal perturbation around ~7.1 Ma.

The ZFT ages in the studied sediments suggest contemporaneous rapid tectonic exhumation, erosion and sedimentation during the Early Miocene time.

The thermal history of the Ibar Basin was controlled by exhumation and cooling of the Studenica and Kopaonik core-complex. The rapid cooling of the Studenica and Kopaonik footwall transferred heat to the basin in the hanging wall. The termination of the heating episode in the hanging wall units and the onset of cooling (10–8 Ma) imply changes in tectonic settings from extension to basin inversion and erosion.

The thermal evolution of the Inner Dinarides was most likely controlled by the Miocene extension accompanied by crustal melting, mass and heat transfer via detachments and/or due to volcanism ± hydrothermal activity.

References

Anđelković M., Eremija M., Pavlović M., Anđelković J. & Mitrović-Petrović J. 1991: Paleogeography of Serbia-Tertiaty. *Univ. Belgrade, Fac. Mining and Geol., Institute for regional geology and paleontology*, 1–237 (in Serbian with English summary).

Barker C.E. & Pawlewicz M.J. 1986: The correlation of vitrinite reflectance with maximum temperature in humic organic matter. In: Buntebarth G. & Stegena L. (Eds.): Paleogeothermics, lecture notes, earth sciences. *Springer-Verlag*, Berlin 5, 79–93.

Brandon M.T. 2002: Decomposition of mixed grain age distributions using BinomFit. *On Track* 24, 13–18.

Brković T., Malešević M., Urošević M., Trifunović S. & Radanović Z. 1976: Basic Geological Map of the SFRY, 1:100,000, Sheet Ivanjica (K34-17). *Federal Geol. Ins. of Yugoslavia*, Belgrade (in Serbian).

Burtner R.L., Nigrini A. & Donelick R.A. 1994: Thermochronology of Lower Cretaceous source rocks in the Idaho-Wyoming thrust belt. *AAPG Bull.* 78, 1613–1636.

Cvetković V. 2002: Nature and origin of pyroclastic deposits of the Miocene Eruptive Complex of Borač (Central Serbia). *Bull CXXV de l' Acad. Serbe des Sci. et des Arts, Classe des Sci. Math. Natur., Sci. Natur.* 342, 209–215.

Cvetković V. & Pécskay Z. 1999: The Early Miocene eruptive complex of Borač (central Serbia): volcanic facies and evolution over time. Extended abstract. *Carpathian Geology 2000, October 11–14, 1999, Smolenice, Geol. Carpathica* 50, 91–93.

Cvetković V., Karamata S. & Knežević-Đorđević V. 1995: Vulcanic rock of the Kopaonik area. [Savetovanje "Geologija i metalogenija Kopaonika"]. *Republički društveni fond za geološka*

istraživanja Srbije, 19–22 jun 1995, 185–195 (in Serbian with English abstract).

Cvetković V., Prelević D., Downes H., Jovanović M., Vaselli O. & Pécskay Z. 2004: Origin and geodynamic significance of Tertiary postcollisional basaltic magmatism in Serbia (Central Balkan Peninsula). *Lithos* 73, 161–186.

de Leeuw A., Mandić O., Krijgsman W., Kuiper K.F. & Hrvatović H. 2012: Paleomagnetic and geochronologic constraints on the geodynamic evolution of the Central Dinarides. *Tectonophysics* 530–531, 286–298.

Dimitrijević M.D. 1997: Geology of Yugoslavia. 2nd ed. *Geoinstitute*, Belgrade, 1–187.

Donelick R.A. 1993: Apatite etching characteristics versus chemical composition. *Nucl. Tracks Radiat. Meas.* 21, 4, 604.

Dunkl I. 2002: Trackkey: a Windows program for calculation and graphical presentation of fission track data. *Computers & Geosciences* 28, 1, 3–12.

Dunkl I., Grasemann B. & Frisch W. 1998: Thermal effects of exhumation of a metamorphic core complex on hanging wall syn-rift sediments — an example from the Rechnitz Window, Eastern Alps. *Tectonophysics* 297, 31–50.

Ercegovac M., Životić D. & Kostić A. 2006: Genetic industrial classification of Brown Coals in Serbia. *Int. J. Coal Geol.* 68, 39–56.

Ercegovac M., Wolf M., Hagemann H.W. & Püttmann W. 1991: Petrological and geochemical studies of the coals of the Ibar River basin (Yugoslavia). *Int. J. Coal Geol.* 19, 145–162 (in German).

Falick A.E., Ilich M. & Russel M.J. 1991: A stabile isotope study of the magnesite deposits associated with the alpine-type ultramafic rocks of Yugoslavia. *Econ. Geol.* 86, 847–861.

Friedmann S.J. & Burbank D.W. 1995: Rift basins and supradetachment basins: Intracontinental extensional end-members. *Basin Res.* 7, 109–127.

Galbraith R.F. 1981: On statistical models for fission track counts. *Mathemathical Geol.* 13, 471–478.

Galbraith R.F. & Green P.F. 1990: Estimating the component ages in a finite mixture. *Nucl. Tracks Radiat. Meas.* 17, 197–206.

Galbraith R.F. & Laslett G.M. 1993: Statistical models for mixed fission track ages. *Nucl. Tracks Radiat. Meas.* 21, 459–470.

Gleadow A.J.W. 1981: Fission-track dating methods — what are the real alternatives. *Nucl. Tracks Radiat. Meas.* 5, 3–14.

Gleadow A.J.W., Duddy I.R., Green P.F. & Hegarty K.A. 1986: Fission track length in the apatite annealing zone and interpretation of mixed ages. *Earth Planet. Sci. Lett.* 78, 245–254.

Grasemann B. & Mancktelow N.S. 1993: Two-dimensional thermal modeling of normal faulting: the Simplon Fault Zone, Central Alps, Switzerland. *Tectonophysics* 255, 65–155.

Green P.F., Duddy I.R., Gleadow A.J.W., Tingate P.R. & Laslett G.M. 1986: Thermal annealing of fission tracks in apatite. 1. A qualitative description. *Chem. Geol.* (*Isotope Geoscience Section*) 59, 237–253.

Harzhauser M. & Mandić O. 2008: Neogene lake systems of Central and South-Eastern Europe: Faunal diversity, gradients and interrelations. *Palaeogeogr. Palaeoclimatol. Palaeoecol.* 260, 417–434.

Horváth F., Bada G., Szafián P., Tari G., Ádám A. & Cloetingh S. 2006: Formation and deformation of the Pannonian Basin: constraints from observational data. *Geol. Soc. London*, *Mem.*, 191–206.

Hurford A.J. & Carter A. 1991: The role of fission track dating in discrimination of provenance. In: Morton A.C., Todd S.P. & Haughton P.D.W. (Eds.): Developments in sedimentary provenance studies. *Geol. Soc. London, Spec. Publ.* 57, 67–78.

Hurford A.J. & Green P.F. 1983: The zeta-age calibration of fission-track dating. *Isotope Geosci.* 1, 285–317.

Ilić A. & Neubauer F. 2005: Tertiary to recent oblique convergence and wrenching of the Central Dinarides: Constraints from a palaeostress study. *Tectonophysics* 410, 465–484.

Karamata S. 2006: The geological development of the Balkan Peninsula related to the approach, collision and compression of Gondwanan and Eurasian units. In: Robertson A.H.F. & Mountrakis D. (Eds.): Tectonic development of the Eastern Mediterranean Region. *Geol. Soc. London, Spec. Publ.* 260, 155–178.

Ketcham R.A. 2005: Forward and inverse modeling of low-temperature thermochronometry data. *Rev. Mineral. Geochem.* 58, 275–314.

Ketcham R.A., Donelick R.A. & Donelick M.B. 2003: AFTSolve: a program for multikinetic modeling of apatite fission-track data. *Amer. Mineralogist* 88, 1–929.

Ketcham R.A., Carter A., Donelick R.A., Barbarand J. & Hurford A.J. 2007: Improved modeling of fission-track annealing in apatite. *Amer. Mineralogist* 92, 799–810.

Kochansky V. & Slisković T. 1981: Jüngere Miozäne Kongerien in Kroatien, Bosnien und Herzegovina. *Paleont. Jugosl.*, Zagreb 19, 1–98.

Kounov A., Seward D., Bernoulli D., Burg J.-P. & Ivanov Z. 2004: Thermotectonic evolution of an extensional dome: the Cenozoic Osogovo-Lisets core complex (Kraishte zone, western Bulgaria). *Int. J. Earth Sci.* 93, 1008–1024.

Krstić N., Savić Lj., Jovanović G. & Bodor E. 2003: Lower Miocene lakes of the Balkan Land. *Acta Geol. Hung.* 46, 291–299.

Krstić N., Dumadzanov N., Olujić J., Vujanović L. & Jankovic-Golubović J. 2001: Interbedded tuff and bentonite in the Neogene lacustrine sediments of the central part of the Balkan Peninsula. A review. *Acta Vulcanol.* 13, 91–99.

Laslett G.M., Green P.F., Duddy I.R. & Gleadow A.J.W. 1987: Thermal annealing of fission tracks in apatite. 2. A quantitative analysis. *Chem. Geol., Isotope Geosci. Section* 65, 1–13.

Lenkey L., Dovenyi P., Horvath F. & Cloetingh S.A.P.L. 2002: Geothermics of the Pannonian basin and its bearing on the Neotectonics. *EGU Stephan Mueller, Spec. Publ. Ser.* 3, 29–40.

Lister G.S. & Davis G.A. 1989: The origin of metamorphic core complexes and detachment faults formed during Tertiary continental extension in the northern Colorado River region, U.S.A. *J. Struct. Geol.* 11, 65–94.

Matenco L. & Radivojević D. 2012: On the formation and evolution of the Pannonian Basin: Constraints derived from the structure of the junction area between the Carpathians and Dinarides. *Tectonics*, 31, TC6007. Doi: 6010.1029/2012tc003206

Márton I., Moritz R. & Spikings R. 2010: Application of low-temperature thermochronology to hydrothermal ore deposits: Formation, preservation and exhumation of epithermal gold systems from the Eastern Rhodopes, Bulgaria. *Tectonophysics* 483, 240–254.

Milivojević M. 1993: Geothermal model of Earth's crust and lithosphere for the territory of Yugoslavia: some tectonic implications. *Stud. Geophys. Geod.*, 37, *Acad. Sci. Czech Republic*, Praha, 265–278.

Mojsilović S., Baklajić D. & Djoković I. 1978: Basic Geological Map of the SFRY, 1:100,000, Sheet Sjenica (K32–29). *Federal Geol. Inst.*, Belgrade.

Obradović J., Stamamakis G.M., Aničić S. & Economy S.G. 1992: Borate and borosilicate deposites in the miocene Jarandol basin, Serbia, Yugoslavia. *Econ. Geol.* 87, 8, 2169–2174.

Pamić J., Tomljenović B. & Balen D. 2002: Geodynamic and petrogenetic evolution of Alpine ophiolites from the central and NW Dinarides: an overview. *Lithos* 65, 113–142.

Prysjazhnjuk V., Kovalenko V. & Krstić N. 2000: On the terrestrial and freshwater molluscs from Neogene of Western Serbia.

Geology and metallogeny of the Dinarides and the Vardar zone. *Proc. Internat. Symp.*, Zvornik, Belgrade, 219–224.

Schefer S. 2010: Tectono-metamorphic and magmatic evolution of the Internal Dinarides (Kopaonik area, southern Serbia) and its significance for the geodynamic evolution of the Balkan Peninsula. *PhD Thesis*, *University of Basel*, Switzerland, 1–242.

Schefer S., Cvetković V., Fügenschuh B., Kounov A., Ovtcharova M., Schaltegger U. & Schmid S.M. 2011: Cenozoic granitoids in the Dinarides of southern Serbia: age of intrusion, isotope geochemistry, exhumation history and significance for the geodynamic evolution of the Balkan Peninsula. *Int. J. Earth Sci.* 100, 1181–1206.

Schefer S., Egli D., Missoni S., Bernoulli D., Fügenschuh B., Gawlick H.J., Jovanović D., Krystyn L., Lein R., Schmid S.M. & Sudar M.N. 2010: Triassic metasediments in the Internal Dinarides (Kopaonik area, southern Serbia): stratigraphy, paleogeographic and tectonic significance. *Geol. Carpathica* 61, 89–109.

Schmid S.M., Bernoulli D., Fügenschuh B., Matenco L., Schefer S., Schuster R., Tischler M. & Ustaszewski K. 2008: The Alpine-Carpathian-Dinaridic orogenic system: correlation and evolution of tectonic units. *Swiss J. Geosci.* 101, 139–183.

Souche A., Beyssac O. & Andersen T.B. 2012: Thermal structure of supra-detachment basins: a case study of the Devonian basins of western Norway. *J. Geol. Soc. London* 169, 427–434.

Stojadinović U., Matenco L., Andriessen P.A.M., Toljić M. & Foeken J.P.T. 2013: The balance between orogenic building and subsequent extension during the Tertiary evolution of the NE Dinarides: Constraints from low-temperature thermochronology. *Global and Planetary Change* 103, 19–38.

Tagami T., Galbraith R.F., Yamada R. & Laslett G.M. 1998: Revised annealing kinetics of fission tracks in zircon and geological implications. In: Van den Haute P. & De Corte F. (Eds.): Advances in fission-track geochronology. *Kluwer Academic Publishers*, Dordrecht, Netherlands, 99–112.

Tari G., Horváth F. & Rumpler J. 1992: Styles of extension in the Pannonian Basin. *Tectonophysics* 208, 203–219.

Tari G., Dövényi P., Dunkl I., Horváth F., Lenkey L., Stefanescu M., Szafián P. & Tóth T. 1999: Lithospheric structure of the Pannonian basin derived from seismic, gravity and geothermal data. In: Durand B., Jolivet F., Horváth F. & Séranne M. (Eds.): The Mediterranean Basins: Tertiary extension within the Alpine Orogen. *Geol. Soc. London*, *Spec. Publ.* 156, 215–250.

Taylor G.H., Teichmüller M., Davis A., Diessel C.F.K., Littke R. & Robert P. 1998: Organic petrology. *Gebrüder Borntraeger*, Berlin, 1–704.

Urošević M., Pavlović Z., Klisić M., Brković T., Malešević M. & Trifunović S. 1970a: Basic Geological Map of the SFRY, 1:100,000, Sheet Novi Pazar (K34–3). *Savezni Geološki Zavod*, Beograd (1966).

Urošević M., Pavlović Z., Klisić M., Brković T., Malešević M. & Trifunović S. 1970b: Basic Geological Map of the SFRY, 1:100,000, Sheet Vrnjci (K34–18). *Savezni Geološki Zavod*, Beograd (1966).

Ustaszewski K., Kounov A., Schmid S.M., Schaltegger U., Krenn E., Frank W. & Fügenschuh B. 2010: Evolution of the Adria–Europe plate boundary in the northern Dinarides from continent-continent collision to back-arc extension. *Tectonics* 29, TC6017. Doi: 10.1029/2010TC002668

Ustaszewski K., Schmid S.M., Lugović B., Schuster R., Schaltegger U., Bernoulli D., Hottinger L., Kounov A., Fügenschuh B. & Schefer S. 2009: Late Cretaceous intra-oceanic magmatism in the internal Dinarides (northern Bosnia and Herzegovina): Implications for the collision of the Adriatic and European plates. *Lithos* 108, 106–125.

Wagner G.A. & Van den Haute P. 1992: Fission-track dating. *Enke Verlag*, Stuttgart, 1–285.

Životić D., Jovančićević B., Schwarzbauer J., Cvetković O., Gržetić I., Ercegovac M., Stojanović K. & Šajnović A. 2010: The petrographical and organic geochemical composition of coal from the East field, Bogovina Basin (Serbia). *Int. J. Coal Geol.* 81, 227–241.

Životić D., Wehner H., Cvetković O., Jovančićević B., Gržetić I., Scheeder G., Vidal A., Šajnović A., Ercegovac M. & Simić V. 2008: Petrological, organic geochemical and geochemical characteristics of coal from the Soko Mine, Serbia. *Int. J. Coal Geol.* 73, 285–306.